International Journal of Heat and Mass Transfer 242 (2025) 126859

Contents lists available at ScienceDirect

International Journal of Heat and Mass Transfer

journal homepage: www.elsevier.com/locate/ijhmt

Heat and mass transfer characteristics of a horizontal tube falling film absorber working with water/lithium bromide and ionic liquid as an anti-crystallization additive

Hussain A. Tariq, Mahmoud Bourouis *, Alberto Coronas

Department of Mechanical Engineering, Universitat Rovira i Virgili, Av. Països Catalans 26, 43007 Tarragona, Spain

ARTICLE INFO

Keywords:
Horizontal tube
Falling film absorber
Absorber thermal conditions
Water/LiBr
Ionic liquids
Anti-crystallization additive
Heat and mass transfer performance

ABSTRACT

Absorption Heat Pumps (AHPs) become attractive when low-grade energy sources power them. The water/LiBr is a commonly used working solution in which water is used as a refrigerant which is economical, abundant, non-toxic and natural refrigerant. However, water/LiBr AHPs faces an inherent challenge in operating at higher concentrations, which restrict their capability for cooling at high heat sink temperatures or for heating applications. LiBr crystallizes in water/LiBr solution at high concentrations, limiting the operational range and affecting the performance of the absorption cycle. Ionic Liquid (IL) can be added as an anti-crystallisation additive to improve the solubility of LiBr in absorbent solution. In this work, 1,3-Dimethyl-1H-imidazolium chloride [DMIM][Cl] is used as an additive containing a 6 % mass fraction in absorbent (LiBr+[DMIM][Cl]). This paper aims to characterise the wettability and heat and mass transfer processes for water/(LiBr+[DMIM][Cl]) and water/LiBr solutions at air- and water-cooling thermal conditions. A horizontal tube falling film absorber is used in the present investigation. The new solution shows no adverse effects on the heat and mass transfer processes compared to water/LiBr; thus, both solutions performed similarly. The increase of 3 %, 8 %, and 3 % on average is noted for water absorption mass flux, heat transfer coefficient and absorber heat duty, respectively, at a cooling water temperature of 50 °C, with solution inlet subcooling of -3 °C and an absorbent concentration of 64 %. Additionally, the new working solution water/LiBr+[DMIM][Cl]) shows better wettability of absorber tube than water/LiBr, which is favorable for the absorption process.

1. Introduction

The demand for cooling is instantly rising due to population, economic growth and climate change. A prediction hints that by 2050, almost two-thirds of households worldwide will be equipped with air conditioning [1]. Likewise fossil fuels are used for residential heating purposes at present. However, the utilization of synthetic refrigerants and fossil fuels are contributing to the greenhouse gases emission and accelerating the global warming. Natural refrigerants and renewable energy resources for heating and cooling indoor spaces can potentially play a substantial role in decreasing the impact of these problems. Unlike from vapor compression technology which consumes more electricity and uses synthetic refrigerants, absorption technology presents an attractive solution for energy and environmental challenges. Absorption chillers are intriguing when powered by low-grade energy sources. This technology's lowered energy consumption and environmentally friendly attributes make it more attractive.

Several working mixtures have been suggested for absorption technology; however, plenty of these have been ended for a variety of reasons, including high cost, high corrosiveness, safety, environmental risks, poor transport qualities or chemical instability. The ammonia and water working solution is one of the most used working pair in industrial absorption refrigeration systems due to the excellent thermodynamic and thermophysical characteristics of ammonia [2]. Despite many advantages of this working pair, it requires higher driving temperatures and a rectifier to successfully separate ammonia and water due to the inherent volatile nature of water. Moreover, toxic nature of ammonia makes it unsuitable for space cooling and heating. It can cause coughing, nose and throat discomfort, while higher concentration can damage the lungs or even leads to death [3]. Another commercially available working pair for space cooling applications is the water/LiBr mixture, where water is the refrigerant (natural), which is affordable and non-toxic in nature [4–7]. Moreover, water/LiBr absorption systems can

* Corresponding author.
E-mail address: mahmoud.bourouis@urv.cat (M. Bourouis).

https://doi.org/10.1016/j.ijheatmasstransfer.2025.126859
Received 20 December 2024; Received in revised form 1 February 2025; Accepted 17 February 2025
Available online 25 February 2025

NOMENCLATURE

A_y	surface area of tube, m^2
B	Refers to particular property
D	pipe diameter, mm
c_p	specific heat capacity, J/kg. °C
$\dot{m}$	mass flow rate, kg/s
$\dot{m}_v$	vapor absorption mass flux, $kg/m^2.s$
L	pipe length, m
n	number of pipes
k	thermal conductivity, W/m.K
$\dot{Q}_{abs}$	absorber heat duty, kW
h	heat transfer coefficient, $kW/m^2.K$
U	overall heat transfer coefficient, $kW/m^2.K$
Un	Uncertainty
T	temperature, °C, K
V	velocity, m/s
ΔT_{lm}	log mean temperature difference, °C
Γ	solution mass flow rate per unit of wetted pipe length, kg/m.s
X	concentration, kg/kg
Nu	Nusselt number
Pr	Prandtl number
Re	Reynolds number
p	pressure, kPa
ρ	density, kg/m^3
μ	viscosity, Ns/m^2, mPa.s

Subscript

c	cooling water
s	solution
i	inlet
in	inner
o	outlet
out	outer
v	vapor
w	water
sat	saturation
ss	stainless steel
SHE	Solution Heat Exchanger

operate at lower activation temperatures and usually require wet cooling batteries for heat dissipation.

Nevertheless, water/LiBr AHPs face a fundamental challenge when operating at higher LiBr concentrations, as this limits their capability for cooling at high heat sink temperatures or for heating applications. However, preferring an air-cooled absorption system can offer greater benefits in terms of less space and maintenance by eliminating the cooling tower. Absorption chillers can be more compact by integrating an air-cooled system. However, the air-cooled absorption chillers are rarely available commercially. LiBr crystallization issue limits the operational range and affects the performance of the absorption cycle. Various ideas have been tested to solve the LiBr crystallization issue in recent years. Addition of chemical crystallization inhibitors and improvement of heat and mass transfer are among the effective strategies to reduce the LiBr crystallization issue [8]. Reimann et al. [9] introduced "Carrol" solution, which contains water/LiBr, ethylene glycol (crystallization inhibitor) and 1-nonylamine (to enhance heat and mass transfer). Although this solution resulted in improvement of solubility and film heat transfer coefficient, but 1-nonylamine was ultimately replaced by phenylmethyl carbinol as it formed chemically refractory copper soaps when heated in the presence of copper oxide. Additionally, because of the presence of ethylene glycol in the vaporized refrigerant from the generator, Inoue [10] and Park et al. [11] suggested adding a rectifier for this working mixture. Bourouis et al. [12] experimentally studied the absorption of water vapour in water/(-LiBr+LiI+$LiNO_3$+LiCl) falling film vertical tube absorber at air-cooling thermal conditions. The new aqueous solution demonstrates lower crystallization temperature and better mass transfer, hence making it beneficial particularly for air-cooled system. Kim et al. [13] evaluated the theoretical COP of three potential working fluid solutions for air-cooled absorption chillers: LiBr+$H_2N(CH_2)_2OH$+H_2O, LiBr+HO$(CH_2)_3OH$+H_2O, and LiBr+$(HOCH_2CH_2)_2NH$+H_2O. They found that LiBr+$H_2N(CH_2)_2OH$+H_2O provided the widest operating range but found various issues involving corrosion, reduced heat and mass transfer performance, and need for a rectifier. Improvement of heat and mass transfer performance of the solution in absorption chillers is also beneficial to reduce the size of the absorption machines. Yoon et al. [14] performed experimental study to investigate the heat and mass transfer performance of falling film LiBr+LiI+$LiNO_3$+LiCl and LiBr aqueous solutions using helical absorber. The heat and mass transfer of LiBr+LiI+$LiNO_3$+LiCl solution was improved up to 5 % as compared to LiBr solution. In an experimental work by Yoon et al. [15], heat transfer was studied by adding the normal octyl alcohol as additive in water/LiBr solution. The experiments were conducted using horizontal tube absorber. The results showed 35–90 % improvement in the heat transfer. Lin et al. [16] added 2-ethyl-1-hexanol as additive in water/LiBr and found the improvement in mass transfer of almost double. They used vertical falling film absorber for their experimental study.

Aiming to improve the solubility of LiBr in water/LiBr solution to address the operational limitations related to this solution, ILs, a distinct category of liquid salts composed of charged particles called ions, gained notable interest in absorption technology [17,18]. They are thermally stable, non-flammable and can exists in liquid phase over a wide range of temperatures. To avoid crystallization problem, Araújo et al. [19] used 1-ethyl-3-methyl-imidazolium ethylsulfate ([EMIM][EtSO4]) and 1-ethyl-3-methyl-imidazolium tetrafluoroborate ([EMIM][BF4]) as absorbents with water as a refrigerant to simulate the performance of absorption refrigeration systems. They found COP and exergy efficiency values for water/[EMIM][EtSO4] solution close to those of water/LiBr solution. Zhang et al. [20] used 1-ethyl-3-methylimidazolium dimethylphosphate ([EMIM][DMP]) as absorbent and water as a refrigerant, to simulate the performance of an absorption chiller. They found a lower performance for new solution comparatively to water/LiBr solution. Królikowska et al. [21,22] studied the impact of various ILs as additives on the solubility of a water/LiBr solution. Their work showed that even a little amount of IL in the water/LiBr solution, substantially improved the solubility of the solution. Latorre et al. [23] reported a study about the quantitative and structural assessment of water association in solutions of water/LiBr-1,3-dimethylimidazolium chloride ([DMIM][Cl]). They found that the quantity of water retained as bulk water in case of addition of additives exceeds in comparison to water/LiBr case.

The absorber maintains a vital importance in the absorption chillers, having a significant impact on the performance, cost, and size. A typical design of absorber is the horizontal tubes falling film, which enables the simultaneous transfer of both heat and mass [24–27]. These horizontal tubes design is the most commonly available in commercial absorption chillers. Wettability is crucial for the absorption process taking place in the absorber. Improved wetting confirms a larger surface area of the absorber tubes are in contact with the working fluid, which is important for effective absorption of the refrigerant vapours. A poor wetting characteristic of the solution may not spread evenly over the absorber tubes. A preferential path on the absorber tubes can lead to the

formation of dry patches, which reduces the effective surface area available for absorption, leading to a lower overall vapor absorption rate. It is often challenging to maintain uniformly distribution of the solution on horizontal tubes of the absorber.

The solubility of LiBr in water/LiBr solution can be improved by adding IL as additive. At air-cooling thermal conditions and in reversible mode for heating application, the operating concentration of LiBr in the strong solution leaving the solution heat exchanger (SHE) is at the verge of crystallization. The absorber is unable to operate at high LiBr concentrations due to this risk; hence, the cycle driving temperature range is limited which compromises the performance of overall system. Therefore, the use of IL as additive becomes significant, thus providing a privilege to operate the cycle at higher temperatures of the driving heat source, thereby enabling the absorber to function at higher absorbent concentrations. In a recent work by CREVER research group in collaboration with LOCIE [28], [DMIM][Cl] (6 % of absorbent mass fraction) was added to water/LiBr solution in an absorption chiller prototype. The operating range of the chiller was improved by adding a small amount of [DMIM][Cl], with negligible impact on the thermal performance of the prototype. Hence, adding [DMIM][Cl] at 6 % mass fraction of absorbent demonstrates better solubility of the absorbent solution without significantly affecting the water/LiBr thermodynamic properties. So, there was a need to study the influence of [DMIM][Cl] in water/LiBr solution on heat and mass transfer performance of the absorber which is the most vital component of the AHPs. In this study, [DMIM][Cl] is added as an additive in water/LiBr solution to determine and compare the heat and mass transfer performance of water/(LiBr+[DMIM][Cl]) solution with the conventional water/LiBr solution. The wettability and heat and mass transfer performance of both solutions are investigated using a typical horizontal tube falling film absorber. This is the most widely used configuration in commercial absorbers. The new solution includes 6 % [DMIM][Cl] by mass as part of the absorbent (LiBr+[DMIM][Cl]). The study is carried out at both water-cooling and air-cooling thermal conditions. To the best of authors knowledge, no experimental study is currently available which reports this comparison. To perform this study, the paper is structured as follows: firstly, the experimental setup used in this study is described in Section 2 followed by the methodology in Section 3. Afterwards, the comparison of experimental data with literature is presented in Section 4, while the results are presented and discussed Section 5. Finally, the key findings are concluded in Section 6.

2. Experimental setup

To study the effect of adding [DMIM][Cl] in water/LiBr solution on wettability and heat and mass transfer processes, a horizontal tube falling film absorber is used. The experimental setup comprises three basic circuits: one for the solution, the other for cooling water, and a third one for the vapor line. The key component under study in the experimental setup is the absorber, which consists of six horizontally aligned stainless-steel pipes connected in series to make a tube as shown in Fig. 2. The solution distributor is placed above the tube, aligned with them to ensure perfect distribution of the solution over the tube. Cooling water circulates through the tube in a crossflow pattern comparative to the solution, while the solution flows co current with the vapor. Two peep hole windows are installed in the absorber so that the flow distribution can be visualized. The design parameters of the absorber are listed in Table 1. The generator is used to generate the vapors, using thermal resistance installed within it, which are then transported to the absorber through vapour line. A storage tank is used to store the condensed water coming out from the absorber in case of raising the concentration of the solution. Two Coriolis Micromotion type mass flow meters are located in the solution circuit at the entrance and exit of the absorber to measure the density, temperature and flow rate of the solution. Two Huber thermal baths are used to control the temperature of the solution and cooling water at inlet of the absorber. Plate heat exchangers are placed to exchange the heat at desired locations. A Rosemount Magnetic tube flowmeter is used to measure the flow rate of cooling water. Two TUTHILL (TEC) pumps are used to regulate the flow from generator to absorber and from absorber to generator. A Mitsubishi inverter is used to adjust the frequency of the two pumps. Aplitex PT100 temperature sensors are used to measure the temperatures at desired locations. A pressure transducer (WIKA) is utilized to determine the pressure of absorber and generator tanks. An Agilent data logger is used to display and record the operational data. A Leybold vacuum pump is used to maintain the vacuum conditions inside the system. A two component TITAN epoxy is applied to paint the inner walls of the absorber to avoid possible corrosion. To provide a clearer insight into the experimental setup, a detailed schematic diagram and workbench are presented in Figs. 3. and 4.

Table 1
Design parameters of the absorber.

Parameter	Value
Total pipes (connected in series to make a tube)	6
Wetted length of a pipe	400 mm
Spacing between pipes	30 mm
Outer diameter of pipe	16 mm
Thickness of pipe	1 mm

The experimental arrangement enables the operation of the absorber in a continuous mode under steady state conditions. In the experiments, steady-state conditions were achieved after 30 min for each independent variable constant. For the data presented in this study, an average of at least 5 min of data is used for each steady-state condition. As an example, Fig. 1 illustrates the cooling water temperature at absorber inlet and outlet for water/LiBr under water cooling thermal conditions at solution flow rate of 0.0125 kg/m.s, as a function of time. Although after 20 min, the curve starts to stabilize, a duration of 30 min was typically selected to ensure that all other variables also reached steady-state conditions.

3. Methodology

The methodology implemented to determine and compare the heat and mass transfer performance of water/(LiBr+[DMIM][Cl]) with water/LiBr solutions using a horizontal tube falling film absorber is reported in this section. The selection of the anti-crystallisation additive and preparation of the new solution is described in Section 3.1. The thermophysical properties of the new solution, water/(LiBr+[DMIM][Cl]), are presented in Section 3.2. Section 3.3 provides detail about the data reduction and the definition of the absorber performance parameters considered in the analysis of the simultaneous heat and mass transfer taking place in the absorption process. The experimental conditions employed in this study are given in Section 3.4. The uncertainty involved in the experimental results is given in Section 3.5.

3.1. Additive selection and solution preparation

During the selection of the most suitable commercial IL as an anti-crystallisation additive for this study, two necessary criteria were adopted. First, the decrease in the crystallization temperature of at least 10 °C with respect to water/LiBr solution at 65 % of absorbent mass fraction, and second, a vapor pressure of the absorbent mixture at identical concentrations close to that of water/LiBr. A working solution with lower vapor pressure is desirable as it indicates a stronger affinity between the water and the absorbent. Therefore, among five distinct ILs in water/LiBr solution (1,3-dimethylimidazolium chloride [DMIM][Cl], 1-Butyl-3-methylimidazolium bromide [BMIM][Br], 1-Butyl-3-methylimidazolium chloride [BMIM][Cl], Tris-(2-hydroxyethyl)-methylammonium methyl sulfate [MN((CH2)2(OH))3][MeSO4], and 1-Butyl-3-methylimidazolium acetate [BMIM][OAc]), [DMIM][Cl] exhibited a decrease of >10 °C in the crystallization temperature and vapor pressure

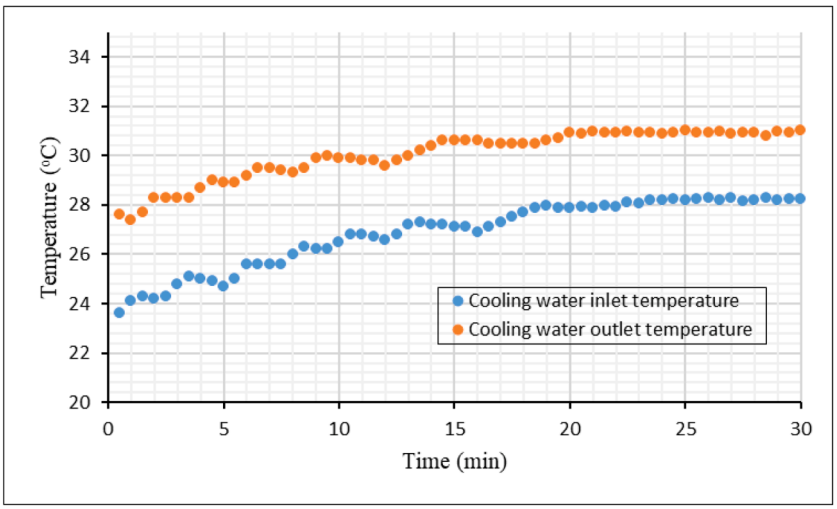

Fig. 1. The variation of temperature over time until steady-state conditions are achieved.

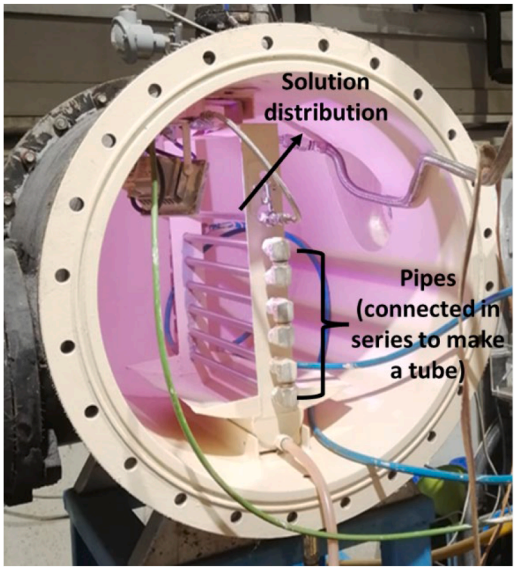

Fig. 2. Horizontal tube falling film absorber (Internal view).

closest to that of the water/LiBr at a mass fraction of 6 % in the absorbent. More detailed information about the selection of the IL is available in [28].

The water/(LiBr+[DMIM][Cl]) solution was then passed through the thermal stability test. The sample was prepared in glass vessel and stirred for 30 min. The solution was divided into two sealed vessels, with one sample maintained at room temperature and the other placed in an oven at 95 °C. The pH and NMR spectra of the prepared samples were analysed after 14 days. The results indicated no significant changes in pH or structure compared to the spectra of the freshly prepared sample. The experiments were repeated after 32 days. The NMR spectra were found to be similar to those of the sample analysed at 14 days. The pH was approximately the same compared to the 14th day sample.

To prepare the new solution, [DMIM][Cl] powder (with 97 % purity) was initially placed within a desiccator (a sealed container linked to vacuum pump) for a duration of two days. The purpose was to eliminate the moisture content if present in the powder. Following this, the required quantity of [DMIM][Cl] mass, equal to 6 % of the absorbent (LiBr+[DMIM][Cl]) concentration, was extracted. In absorbent (LiBr+[DMIM][Cl]), the mass fraction of 6 % is attributed to [DMIM][Cl] while the remaining 94 % consists of LiBr. Prior to depositing the powder into the tray, it was thoroughly cleaned. In the final step, [DMIM][Cl] was added into the water/LiBr solution while maintaining continuous stirring, resulting in the formulation of the new solution water/(LiBr+[DMIM][Cl]). The new solution includes [DMIM][Cl] as part of the absorbent, along with LiBr.

3.2. *Thermophysical properties of new solution*

The properties of the new solution water/(LiBr+[DMIM][Cl]) were determined experimentally in the CREVER research group [28] [30]. The solubility temperatures in the absorbent mass fraction range of 0.58 to 0.69 for water/LiBr and water/(LiBr+[DMIM][Cl]) solutions are presented in reference [28]. In absorption heat pumps, the absorber solution inlet is the critical location for LiBr crystallization. This occurs because the temperature drops after the solution heat exchanger (SHX), and the solution exhibits a high concentration of absorbent. A decrease of 15 °C in the crystallization temperature for water/(LiBr+[DMIM][Cl]) solution in comparison to water/LiBr at 65 % of absorbent mass fraction was noted. This clearly indicates the potential benefit of adding [DMIM][Cl] to water/LiBr solution, as it significantly improves the solubility range of the solution and provides a greater safety margin against crystallization. The improvement in solubility can enable the absorption chiller to operate at high LiBr concentrations that are required for dissipating heat in the absorber and condenser at high temperatures, thus removing the necessity of a direct-contact cooling tower and can enable to operate reversibly for heating applications. The properties of the solution water/(LiBr+[DMIM][Cl]) including density, viscosity, specific heat capacity and vapor pressure at absorber inlet conditions are provided in

Table 2. The plots for all the properties of the new solution over a wide range of mass fraction and temperatures are provided in reference [28]. The density of the solution water/(LiBr+[DMIM][Cl]) is found lower as compared to that of water/LiBr solution. A lower density of the solution indicates that it is closer to the density of the water in comparison to water/LiBr solution. Viscosity of the water/(LiBr+[DMIM][Cl]) solution is higher as compared to that of water/LiBr solution at 64 % mass fraction. The specific heat capacity of the solution water/(LiBr+[DMIM][Cl]) is higher as compared to that of water/LiBr solution. This can be favorable regarding heat and mass transfer perspective as a solution with higher heat capacity can absorb more heat without significant temperature rise, resulting in a lower solution film temperature at the absorber tube in comparison to the solution with lower heat capacity. The vapor pressure of water/(LiBr+[DMIM][Cl]) solution at saturated temperature and mass fraction of absorber inlet conditions is provided in Table 2. At identical mass fractions, the vapor pressure is

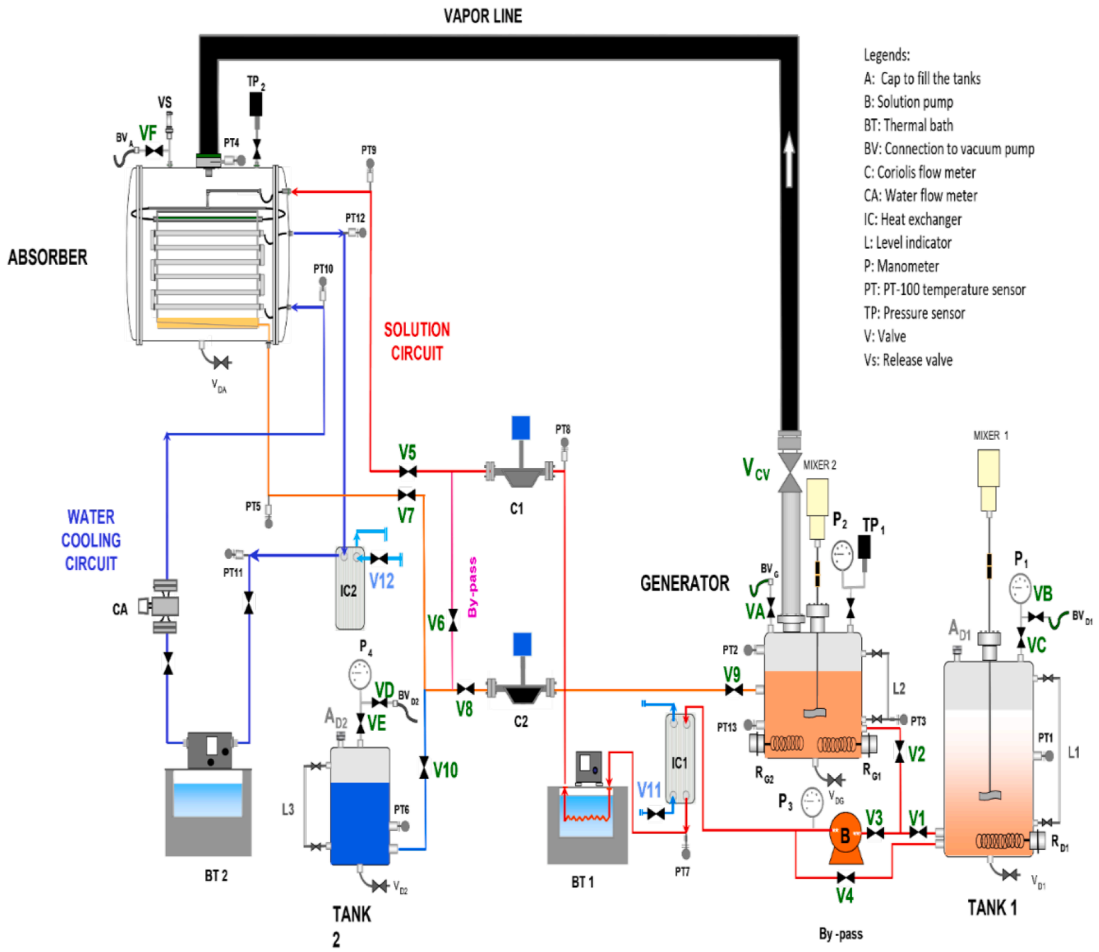

Fig. 3. Experimental setup schematic (adapted from ref [29]).

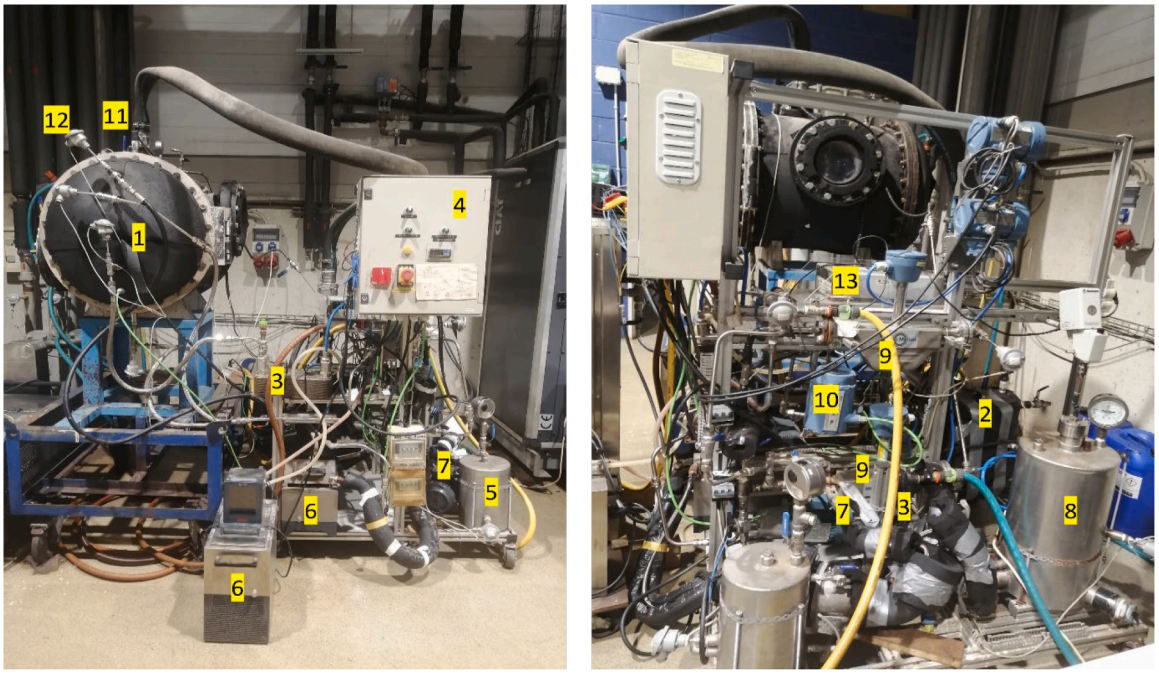

Fig. 4. Experimental workbench. (1) Absorber, (2) Generator, (3) Plate heat exchangers, (4) Control Panel, (5) Storage tank, (6) Thermal baths, (7) Pumps, (8) Preparation tank, (9) Coriolis meters, (10) Flowmeter, (11) Pressure sensor, (12) Temperature sensor and (13) Data logger.

Table 2
Properties of water/LiBr and water/(94 %LiBr+6 % [DMIM][Cl]) solutions.

water/(LiBr+[DMIM][Cl])	water/LiBr [31]	Relative percentage difference $\Delta = \frac{B_{water/LiBr} - B_{water/(LiBr+[DMIM][Cl])}}{B_{water/LiBr}}$
Density (kg.m^{-3})		
ρ (T = 51.0 °C, X = 61 %) = 1630	ρ (T = 53.0 °C, X = 61 %) = 1721	5 %
ρ (T = 55.5 °C, X = 64 %) = 1698	ρ (T = 60.0 °C, X = 64 %) = 1780	4 %
Dynamic viscosity (mPa.s)		
μ (T = 51.0 °C, X = 61 %) = 4.11	μ (T = 53.0 °C, X = 61 %) = 4.55	9 %
μ (T = 55.5 °C, X = 64 %) = 6.02	μ (T = 60.0 °C, X = 64 %) = 5.27	14 %
Isobaric specific heat capacity (kJ/kg. °C)		
C_p (T = 51.0 °C, X = 61 %) = 2.11	C_p (T = 53.0 °C, X = 61 %) = 1.88	12 %
C_p (T = 55.5 °C, X = 64 %) = 2.06	C_p (T = 60.0 °C, X = 64 %) = 1.80	15 %
Vapor pressure (kPa)		
p (T = 51.0 °C, X = 61 %) = 1.3	p (T = 53.0 °C, X = 61 %) = 1.3	–
p (T = 55.5 °C, X = 64 %) = 1.3	p (T = 60.0 °C, X = 64 %) = 1.3	–

kept same for both solutions to compute the saturated temperatures ensuring the same subcooling at the absorber inlet. Therefore, both the solutions will have same potential to absorb the vapors.

3.3. Data reduction

The measured variables, as listed in Table 3 are used to calculate the parameters essential for the analysis of heat and mass transfer governing the absorption process. These parameters are calculated as follows:

The absorbed vapor mass flow rate is determined by applying the mass balances at the absorber:

$$\dot{m}_{s,i} + \dot{m}_v = \dot{m}_{s,o} \tag{1}$$

$$\dot{m}_{s,i} \,.X_i = \; X_o \;.\; \left(\dot{m}_{s,i} + \dot{m}_v\right) \tag{2}$$

The absorber heat duty is calculated using the subsequent equation:

$$\dot{Q}_{abs} = \dot{m}_w \;.c_{p,w} \;.\left(T_{w,o} - T_{w,i}\right) \tag{3}$$

The overall heat transfer coefficient is calculated using the following equation:

$$U = \frac{\dot{Q}_{abs}}{A_y \;.\Delta T_{lm}} \tag{4}$$

where A_y represents the outer surface area of tube

$$A_y = \Pi \;.D_{out} \;.L \;.n \tag{5}$$

The logarithmic mean temperature difference ΔT_{lm} is calculated using the following equation [26]:

$$\Delta T_{lm} = \frac{\left(T_{s,i} - T_{w,o}\right) - \left(T_{s,o} - T_{w,i}\right)}{\ln \frac{\left(T_{s,i} - T_{w,o}\right)}{\left(T_{s,o} - T_{w,i}\right)}} \tag{6}$$

Table 3
Variables measured from experimental setup.

Variables	Locations in Fig. 3
Temperatures	PT5, PT9, PT10, PT12
Pressures	TP1, TP2
Flow rates	C1, C2, CA
Densities	C1, C2

The heat transfer coefficient on the solution side is determined as follows:

$$h_s = \left(\frac{1}{U} - \frac{D_{out} \cdot \left(ln \frac{D_{out}}{D_{in}}\right)}{2.k_{ss}} - \frac{D_{out}}{D_{in}.h_w}\right)^{-1} \tag{7}$$

Using the Dittus-Boelter correlation, the heat transfer coefficient of the cooling water is determined using the following equation [32]:

$$Nu = \frac{h_w.D_{in}}{k_w} = 0.023.Re_w^{0.8}.Pr_w^{0.4} \tag{8}$$

The Reynolds Number for cooling water is calculated as follows:

$$\mathrm{Re}_w = \frac{V_w D_{in} \rho_w}{\mu_w} \tag{9}$$

The solution mass flow rate per unit length is calculated using the subsequent equation:

$$\Gamma_s = \frac{\dot{m}_s}{2.L} \tag{10}$$

Reynolds number of the solution film is calculated using following equation:

$$\mathrm{Re}_{film} = \frac{4.\Gamma_s}{\mu} \tag{11}$$

3.4. Operating conditions used in the experiments

The experimental setup was controlled to deliver the actual operating conditions of the absorber when integrated in a single-effect absorption cycle with heat dissipation at both air-cooling and water-cooling thermal conditions. The operating conditions selected in the present study, as presented in Table 4, are in the range reported by several researchers [33] for typical horizontal tube falling film absorbers.

3.5. Uncertainty analysis

The uncertainty analysis was performed for the calculated parameters necessary for the analysis of heat and mass transfer processes associated with the instrument's uncertainty. The accuracy of 4 wires temperature sensor PT-100 was ±0.02 °C, while the accuracy in Coriolis flow meter was ±0.01 °C in temperature, ±2 kg/m^3 in density and ±0.2 % in flow measurements. The accuracy of Rosemount Magnetic tube flowmeter was ±0.25 % full scale. The uncertainty in parameters was calculated using Root Sum Square method (Eq. (12)), proposed by Kline & McClintock [34].

$$Un(Y) = \left(\left(\sum_i \left(\frac{\partial Y}{\partial x_i} err(x_i)\right)\right)^2\right)^{\frac{1}{2}} \tag{12}$$

Where, Un(Y) is uncertainty in parameter Y, which is function of number of independent variables (x_i). The uncertainty at each point is shown in

Table 4
Operational range applied in this study.

	Air-cooling thermal conditions	Water-cooling thermal conditions
Pressure	1.3 kPa	
Solution inlet subcooling	−2 to −3 °C	4 °C
Solution mass flow rate per unit length of pipe	0.0121–0.0225 kg/m.s, (Re_{film} 8–20)	
Cooling water inlet temperature	40 °C to 50 °C	28 °C to 31 °C
Cooling water flow rate	229 l/h, (0.0636 kg/s), (Re_w 11,000–17,000)	
Concentration	64 %	61 %

the plots in positive and negative directions.

4. Comparison of experimental data with literature

Most experimental investigations on horizontal tube falling film absorbers reported in the open literature focus on the heat and mass transfer processes using water/LiBr as the working fluid. There is no published data for the use of [DMIM][Cl] as an additive in water/LiBr solution. For this reason, a comparison was carried out in the case of water/LiBr solution with horizontal tube falling film absorbers having nearly similar design and operating conditions to the present investigation. A comparison between previous studies [26,35] and the current study is provided in Table 5. In both studies, solution distributor was placed at the top of the horizontal tube and the solution flows from the top to bottom to wet the tube. The cooling water flow was in a crossflow direction relative to the solution flow. The tube was connected in series within a single column. The design specifications are given in Table 5. The values obtained for the refrigerant absorption mass flux, heat transfer coefficient on the solution side, and absorber heat duty in the current study are in the range comparing to the results of Yoon et al. [26] and Kyung et al. [35], with a few exceptions. For instance, a difference of 5 % on average is noted in refrigerant absorption mass flux by increasing the solution flow rate 0.0156–0.0225 kg/m.s (Re_{film}13–20) as compared to the results of Yoon et al. [26]. Similarly, the difference in absorber heat duty is found 10 % on average by increasing the solution flow rate 0.0156–0.0225 kg/m.s as compared to data reported by Kyung et al. [35]. This deviation might be due to few variations in the design of the absorber and experimental operating conditions.

5. Results and discussion

The results are presented and discussed in this section to compare water/LiBr and water/(LiBr+[DMIM][Cl]) solutions used in the horizontal tube falling film absorber at both air-cooling and water-cooling thermal conditions. The comparison is focused on: (i) flow pattern of the solution over the horizontal tube, and (ii) heat and mass transfer involved in the absorption process. The analysis is carried out with the addition of 6 % [DMIM][Cl] mass fraction in the absorbent (LiBr+[DMIM][Cl]). The operating conditions considered in this work are reported in Table 4.

Table 5
Comparison of experimental data of current study with literature.

	Kyung et al. [35]	Yoon et al. [26]	Current study
Concentration of LiBr (%)	60	61	61
Water flow rate (kg/s)	1.262×10^{-4} m^3/s	V_w=1.2 m/s	0.0636 (V_w= 0.7 m/s)
Solution flow rate (kg/m.s)	0.01 – 0.049 Re_{film} (11 – 37)	0.014 – 0.03 Re_{film} (12 – 25)	0.01215 – 0.02257 Re_{film} (10 – 20)
Solution inlet temperature (°C)	47 (sub cooling at inlet 0 °C)	47	48 (sub cooling at inlet 4 °C)
Cooling water inlet temperature (°C)	30	32	28 – 31
Water absorption mass flux (kg/s.m^2)		0.00212 – 0.00276	0.00168 – 0.00241
Heat transfer coefficient (kW/m^2.K)	0.72 – 1.142		1.02 – 1.34
Absorber heat duty (kW)	0.698 – 1.062		0.646 – 0.768
Design specifications	1 Column 4 Rows L = 0.36 m d = 19.05 mm	1 Column 10–16 Rows d = 9.52–15.88 mm	1 Column 6 Rows L = 0.4 m d = 16 mm

5.1. Solution flow over horizontal tube

The solution flow distribution over the horizontal tube of the absorber is shown in Fig. 5. At low solution flow rates (i.e. 0.0121 kg/m.s or Re_{film}=10), droplet fall flow pattern is more noticeable as compared to high solution flow rates (i.e. 0.0225 kg/m.s or Re_{film}=20). During the entire experimental campaign, significant attention was given to address dry patches. Every test was conducted under conditions where no dry patches were present on the tube. If there was any occurrence of a dry patch, it was eliminated timely by adjusting the flow rate. However, dry patches were noted while observing the absorption process over an extended duration, mainly at low solution flow rates as shown in Fig. 5. The presence of these dry patches can affect the absorption process because a significant portion of the tube's effective surface area is inactive in terms of absorption. It was interesting to observe that these patches were less common while using the new solution water/(LiBr+[DMIM][Cl]) as compared to water/LiBr solution. This can be attributed to the lower surface tension of the new solution, which was noted as 82 mN/m, compared to 91 mN/m for water/LiBr solution, at 60 % absorbent mass fraction and 22 °C of temperature, perhaps can improve the wettability of the tube, leading to avoid the formation of preferential paths. Another possibility can be, when there is an uneven distribution or concentration gradients in the absorbent solution, it can lead to the crystallization of LiBr in specific areas, resulting in the appearance of dry patches on the tube surfaces. This phenomenon is more likely to occur at higher concentrations of LiBr. It is noteworthy that the utilization of water/(LiBr+[DMIM][Cl]) solution results in improved wettability considering absorption over prolonged periods at higher absorbent concentrations.

5.2. Heat and mass transfer

In this section, heat and mass transfer characteristics of water/(LiBr+[DMIM][Cl]) and water/LiBr solutions in a horizontal tube falling film absorber are analysed at both air-cooling and water-cooling thermal conditions. Water absorption mass flux, solution heat transfer coefficient, and absorber heat duty are considered as efficiency parameters.

5.2.1. Water absorption mass flux

Water absorption mass flux versus solution flow rate is shown in Fig. 6 at air-cooling thermal conditions. It increases with an increase of the solution flow rate, which was expected as more solution will be in contact with the vapors to absorb them. The water absorption mass flux at $T_{c,i} = 40$ °C is found higher as compared to $T_{c,i} = 50$ °C for both water/(LiBr+[DMIM][Cl]) and water/LiBr solutions. For instance, water absorption mass flux is found 0.00225 kg/m^2.s and 0.00195 kg/m^2.s for water/(LiBr+[DMIM][Cl]) solution at $T_{c,i}$ = 40 °C and $T_{c,i}$ = 50 °C respectively, at 0.0191 kg/s.m (Re_{film} =13) solution flow rate. A lower inlet cooling water temperature helps to maintain a lower temperature of the solution film on the absorber tube surface. This enhances the solution's ability to absorb more water vapor at film interface to reach equilibrium. Moreover, water absorption mass fluxes are found to be slightly higher for water/(LiBr+[DMIM][Cl]) as compared to water/LiBr. This is found 5 %, 3 % and 3 % higher (on average) for water/(LiBr+[DMIM][Cl]) as compared to water/LiBr solution at $T_{c,i} = 40$ °C, $T_{c,i} = 45$ °C and $T_{c,i} = 50$ °C, respectively. As the subcooling at the inlet is same for both the solutions, the potential to absorb vapors is same. The improvement in wettability as explained in Section 5.1 can be the reason for this increase. Another reason for this increase can be related to the higher specific heat capacity of water/(LiBr+[DMIM][Cl]) as compared to water/LiBr solution at identical mass fraction of 64 %, as listed in Table 2. A solution with higher heat capacity can absorb more heat without significant temperature rise, resulting in a lower solution film temperature on the absorber tube surface in comparison to the solution with lower heat capacity. Hence this enhances the solution's ability to absorb more water vapor at film interface to reach equilibrium.

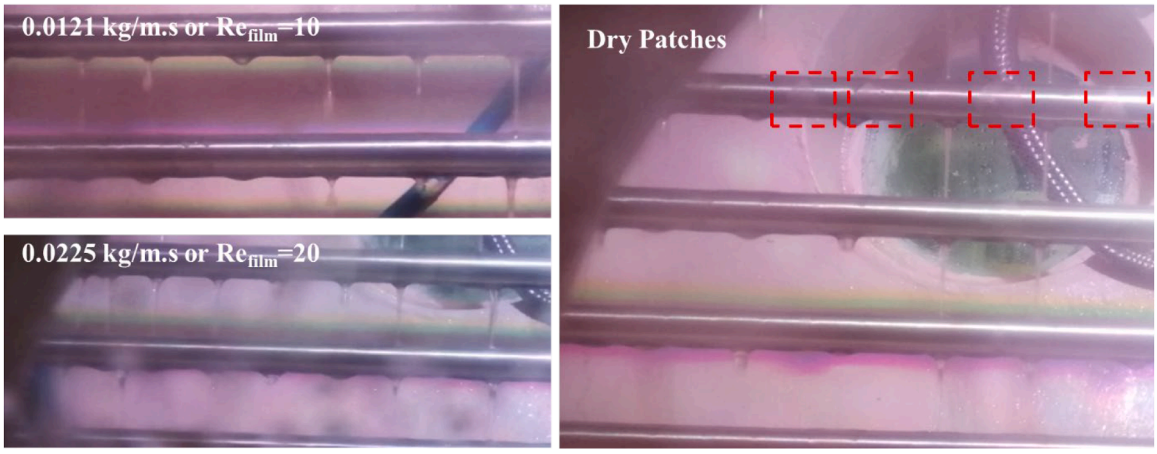

Fig. 5. Solution distribution on horizontal tube.

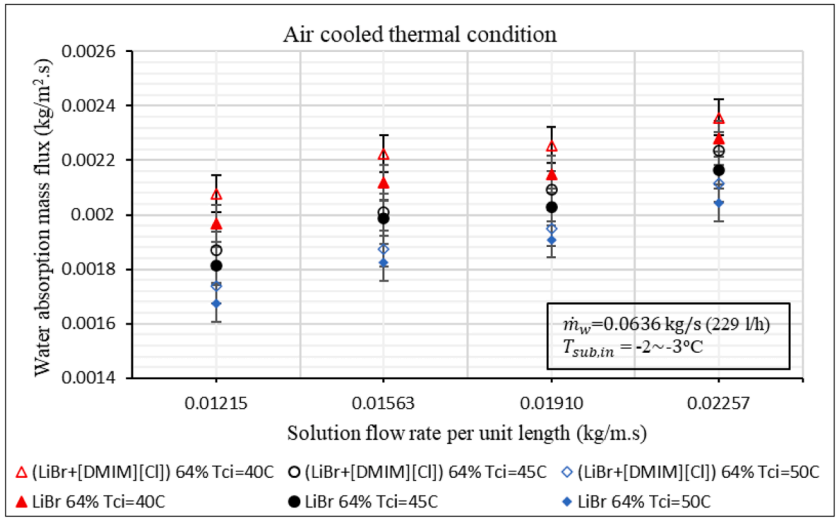

Fig. 6. Water absorption mass flux at air-cooling thermal conditions.

Similarly, at water-cooling thermal conditions, the water absorption mass flux is higher at $T_{c,i} = 28$ °C as compared to $T_{c,i} = 31$ °C (as shown in Fig. 7). It is because of the same reason as explained earlier. Moreover, the water absorption mass flux is found marginally higher for water/(LiBr+[DMIM][Cl]) as compared to water/LiBr, which is 2 % and 3 % on average. It can be due to the better wetting of the tube and higher

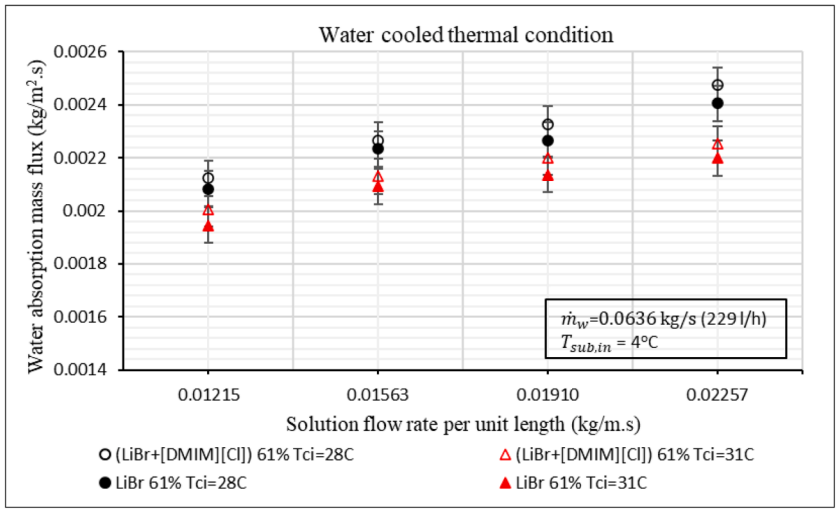

Fig. 7. Water absorption mass flux at water-cooling thermal conditions.

specific heat capacity of water/(LiBr+[DMIM][Cl]) solution as explained earlier. It can be noted that at both air-cooling and water-cooling thermal conditions, although there is a slight increase in water absorption mass flux by adding [DMIM][Cl] as anti-crystallisation additive in water/LiBr solution, it is notable that the new solution shows no adverse effects on the water absorption mass flux.

5.2.2. Solution heat transfer coefficient

As shown in Fig. 8, the solution side heat transfer coefficient increases with an increase of the solution flow rate at air-cooling thermal conditions. It was expected as higher solution flow rate results in improved wetting of the surface of tube inside the absorber. Hence, heat transfer is enhanced as contact area between the solution and absorber tube surface increases. The solution heat transfer coefficient is found higher at $T_{c,i}$ = 50 °C as compared to $T_{c,i}$ = 40 °C. For instance, heat transfer coefficient is found 2.427 kW/m^2.K and 1.292kW/m^2.K for water/(LiBr+[DMIM][Cl]) solution at $T_{c,i}$ = 50 °C and $T_{c,i}$ = 40 °C, respectively, at 0.0156 kg/s.m (Re_{film} =11) solution flow rate. It can be explained by transport property, viscosity. The viscosity of the solution is higher at lower solution temperature and is lower at higher solution temperatures (can be seen in reference [28]). Therefore, at $T_{c,i}$ = 50 °C, the solution film temperature would be higher in comparison to $T_{c,i}$ = 40 °C. Higher solution film temperature corresponds to lower viscosity of the solution, which leads to thinner thermal boundary layer and facilitates better heat transfer from the solution to the tube's wall. Moreover, the solution heat transfer coefficient of new solution water/(LiBr+[DMIM][Cl]) is found higher as compared to water/LiBr. It is 14 %, 9 % and 8 % higher (on average) at $T_{c,i}$ = 40 °C, $T_{c,i}$ = 45 °C and $T_{c,i}$ = 50 °C, respectively. This can be explained due to the better wettability of the water/(LiBr+[DMIM][Cl]) solution as compared to water/LiBr as explained in Section 5.1.

Likewise, the solution heat transfer coefficient at water-cooling thermal conditions, is found higher at $T_{c,i}$ = 31 °C as compared to at $T_{c,i}$ = 28 °C (Fig. 9). The reason is the same as described above in this section. Moreover, it is also found that the solution heat transfer coefficient of water/(LiBr+[DMIM][Cl]) is higher as compared to water/LiBr. It is 6 % higher on average at $T_{c,i}$ = 28 °C and $T_{c,i}$ = 31 °C. It is noted that the heat transfer coefficient of the new solution water/(LiBr+[DMIM][Cl]) is found higher as compared to water/LiBr at both air-cooling and water-cooling thermal conditions.

5.2.3. Absorber heat duty

As shown in Fig. 10, the absorber heat duty increases with solution flow rate at air-cooling thermal conditions. It was expected as more water vapor can be absorbed at higher solution flow rates, which results in more heat being released that needs to be removed. The absorber heat duty is found higher at $T_{c,i}$ = 40 °C as compared to $T_{c,i}$ = 50 °C. For instance, absorber heat duty is found 0.89 kW and 0.66 kW for water/(LiBr+[DMIM][Cl]) solution at $T_{c,i}$ = 40 °C and $T_{c,i}$ = 50 °C respectively, at 0.0156 kg/s.m (Re_{film} =11) solution flow rate. It was expected as absorber heat duty is directly related to water absorption mass flux. Moreover, the absorber heat duty of the new solution water/(LiBr+[DMIM][Cl]) is found higher as compared to water/LiBr. It is 6 %, 4 % and 3 % higher (on average) at $T_{c,i}$ = 40 °C, $T_{c,i}$ = 45 °C and $T_{c,i}$ = 50 °C, respectively. It is due to the higher water absorption mass flux for water/(LiBr+[DMIM][Cl]) solution compared to water/LiBr. The reason for higher water absorption mass flux is explained earlier in Section 5.2.1.

Similarly, at water-cooling thermal conditions, the absorber heat duty is higher at $T_{c,i}$ = 28 °C as compared to $T_{c,i}$ = 31 °C, as shown in Fig. 11. The reason is that the water absorption mass flux is higher at $T_{c,i}$ = 28 °C as compared to $T_{c,i}$ = 31 °C. It is 3 % and 4 % higher (on average) at $T_{c,i}$ = 28 °C and $T_{c,i}$ = 31 °C, respectively. Despite the small increase in the absorber heat duty, it is significant that the new solution water/(LiBr+[DMIM][Cl]) performed quite similar compared to the conventional water/LiBr at both air-cooling and water-cooling thermal conditions.

6. Conclusions

In this work, water/(LiBr+[DMIM][Cl]) and water/LiBr solutions used in horizontal tube falling film absorber are compared based on their heat and mass transfer characteristics. The role of [DMIM][Cl] is as an anti-crystallization agent. The main findings are herein summarized:

- The wettability of horizontal tube was better for water/(LiBr+[DMIM][Cl]) solution as compared to water/LiBr, which is beneficial for longer term operation of the absorber.
- The heat and mass transfer parameters indicated that the new solution water/(LiBr+[DMIM][Cl]) performed similar (marginally better) in comparison with water/LiBr solution, hence the addition of small amount of [DMIM][Cl] had no adverse effects which is the key finding of this work. Whereas the addition of [DMIM][Cl] provides a significant improvement in the solubility which was demonstrated in previous CREVER research work. A decrease of 15 °C in the crystallization temperature for water/(LiBr+[DMIM][Cl]) solution in comparison to water/LiBr at 65 % of absorbent mass fraction was noted. The improvement in solubility is beneficial for absorption heat pumps operating in cooling mode at air-cooling thermal conditions or in heating mode, which requires high absorbent concentrations in the solution circuit. Air-cooled absorption systems have significant benefits, including their compact size due to the absence of cooling towers and associated infrastructure, as well as lower

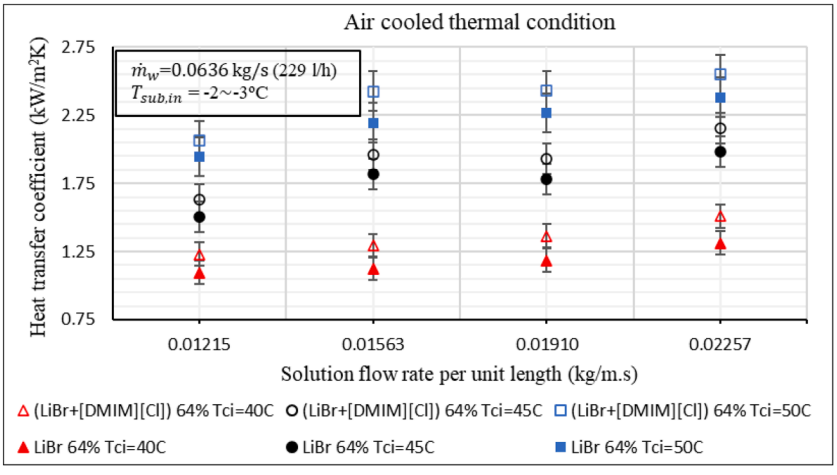

Fig. 8. Solution heat transfer coefficient at air-cooling thermal conditions.

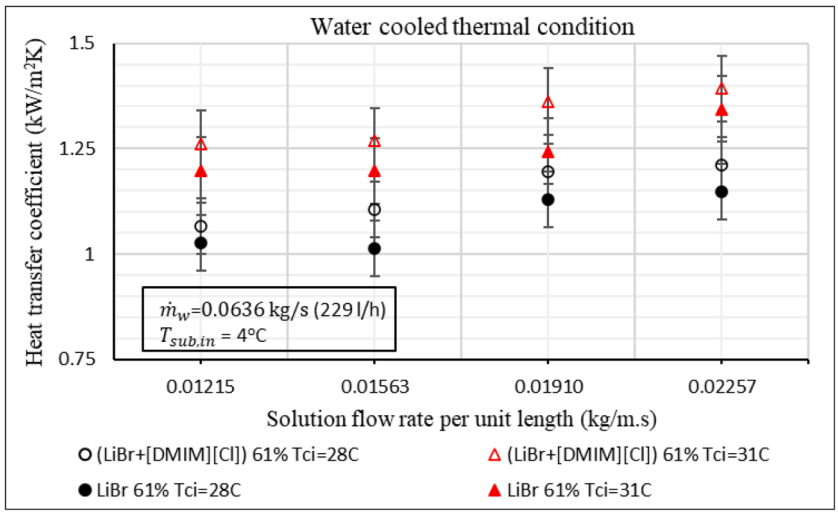

Fig. 9. Solution heat transfer coefficient at water-cooling thermal conditions.

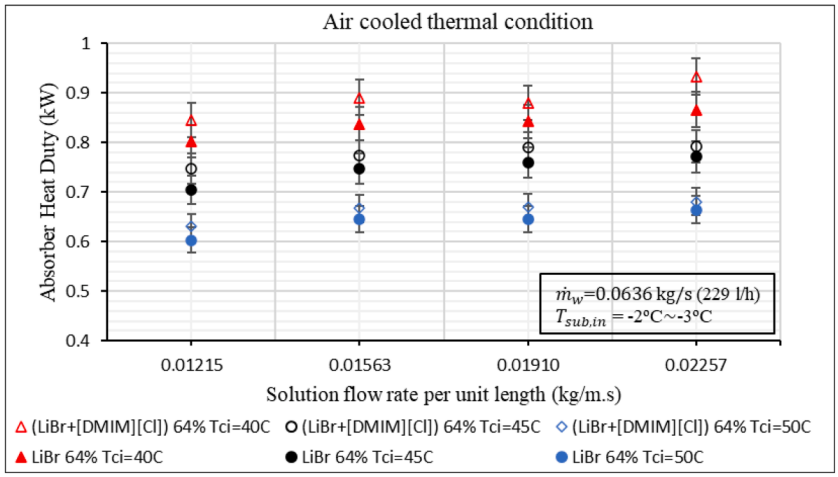

Fig. 10. Absorber heat duty at air-cooling thermal conditions.

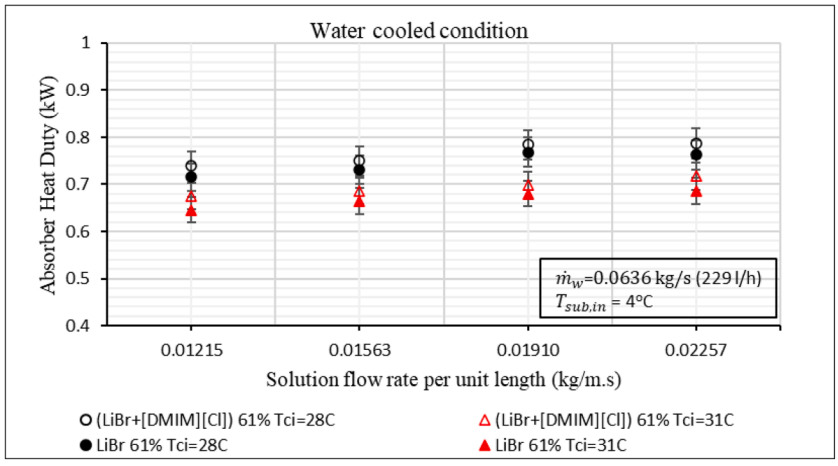

Fig. 11. Absorber heat duty at water-cooling thermal conditions.

maintenance and operational costs. Furthermore, the improvement in solubility allows to work with higher effectiveness of solution heat exchangers, which can improve the overall COP of the absorption cycle.

- Water absorption mass flux was found to be slightly higher for water/(LiBr+[DMIM][Cl]) as compared to water/LiBr at both air-cooling and water-cooling thermal conditions. The maximum increase of 5 % was noted at $T_{c,i} = 40$ °C. The solution side heat transfer coefficient

was found higher for water/(LiBr+[DMIM][Cl]) as compared to water/LiBr at both air-cooling and water-cooling thermal conditions. The maximum increase of 14 % was noted at $T_{c,i} = 40$ °C. The absorber heat duty was found higher for water/(LiBr+[DMIM][Cl]) as compared to water/LiBr at both air-cooling and water-cooling thermal conditions. The maximum increase of 6 % was noted at $T_{c,i} = 40$ °C.

CRediT authorship contribution statement

Hussain A. Tariq: Writing – review & editing, Writing – original draft, Visualization, Validation, Software, Methodology, Investigation, Formal analysis, Data curation. **Mahmoud Bourouis:** Writing – review & editing, Visualization, Validation, Supervision, Resources, Project administration, Methodology, Investigation, Funding acquisition, Formal analysis, Conceptualization. **Alberto Coronas:** Writing – review & editing, Supervision, Resources, Project administration, Investigation, Funding acquisition, Formal analysis, Conceptualization.

Declaration of competing interest

The authors declare the following financial interests/personal relationships which may be considered as potential competing interests:

Mahmoud Bourouis reports financial support was provided by Spain Ministry of Science, Innovation and Universities (MCIN). Alberto Coronas reports financial support was provided by European Union. If there are other authors, they declare that they have no known competing financial interests or personal relationships that could have appeared to influence the work reported in this paper.

Acknowledgements

This study is part of project “PID2020–119004RB-C21”, financed by Spanish Ministry MCIN/AEI/10.13039/501100011033/ and received funding from European Union’s Horizon 2020 research and innovation program under the Marie Skłodowska-Curie grant agreement No 945413 and from the Universitat Rovira i Virgili.

The authors also want to acknowledge YTC America for their funding regarding the measurements of properties of the ([DMIM][Cl]+LiBr)/water solution. We also want to acknowledge Dr. Daniel Salavera for measuring the properties of water/(LiBr+[DMIM][Cl]) solution.

Data availability

Data will be made available on request.

References

[1] "International Energy Agency (IEA), Annual Report 2018 Solar Heating and Cooling Programme, International Energy Agency, Paris, France, 2019.
[2] G. Kini, S. Garimella, Surfactant-enhanced ammonia-water bubble absorption, Int. J. Heat Mass Transfer 187 (2022) 122520, https://doi.org/10.1016/j.ijheatmasstransfer.2022.122520.
[3] "NewYork State", [Online]. Available: https://www.health.ny.gov/environmental/emergency/chemical_terrorism/ammonia_general.htm. [Accessed 04 04 2023].
[4] Y. Kang, H. Kim, K. Lee, Heat and mass transfer enhancement of binary nanofluids for H2O/LiBr falling film absorption process, Int. J. Refrig. 31 (2008) 850–856, https://doi.org/10.1016/j.ijrefrig.2007.10.008.
[5] R. Havestini, S. Ormiston, Detailed two-phase numerical analysis of falling film absorption over a horizontal tube, Int. J. Heat Mass Transfer 198 (2022) 123378, https://doi.org/10.1016/j.ijheatmasstransfer.2022.123378.
[6] A. Mahamoudou, J. Ramousse, N. Pierrès, Analysis of a falling film H2O/LiBr absorber at local scale based on entropy generation, Int. J. Heat Mass Transfer 198 (2022) 123425, https://doi.org/10.1016/j.ijheatmasstransfer.2022.123425.
[7] D.Makarim Pranowo, A. Suami, A. Wijayanta, N. Kobayashi, Y. Itaya, Marangoni convection within thermosolute and absorptive aqueous LiBr solution, Int. J. Heat Mass Transfer 188 (2022) 122621, https://doi.org/10.1016/j.ijheatmasstransfer.2022.122621.
[8] K. Wang, O. Abdelaziz, P. Kisari, E. Vineyard, State-of-the-art review on crystallization control technologies for water/LiBr absorption heat pumps, Int. J. Refrig. 34 (6) (2011) 1325–1337, https://doi.org/10.1016/j.ijrefrig.2011.04.006.
[9] R. Reimann, "Properties of the carrol system and a machine design for solar powered, air cooled, absorption space cooling", *Report No. DOE/CS/31587-T2,* 1981.
[10] N. Inoue, H2O/LiBr+C2H2(OH)2 system and H2O/LiBr+ZnCl2 system, Reito 68 (1993) 719–723.
[11] Y. Park, J. Kim, H. Lee, Physical properties of the lithium bromide+1,3-propanediol+water system, Int. J. Refrig. 20 (5) (1997) 319–325, https://doi.org/10.1016/S0140-7007(97)00021-2.
[12] M. Bourouis, M. Vallès, M. Medrano, A. Coronas, Absorption of water vapour in the falling film of water–(LiBr + LiI + LiNO3 + LiCl) in a vertical tube at air-cooling thermal conditions", Int. J. Thermal Sci. 44 (5) (2005) 491–498, https://doi.org/10.1016/j.ijthermalsci.2004.11.009.
[13] J. Kim, Y. Park, H. Lee, Performance evaluation of absorption chiller using LiBr+H2N(CH2)2OH+H2O, LiBr+HO(CH2)3OH+H2O and LiBr+(HOCH2CH2)2NH+H2O as working fluids, Appl. Therm. Eng. 19 (2) (1999) 217–225, https://doi.org/10.1016/S1359-4311(98)00032-5.
[14] J. Yoon, O. Kwon, C. Moon, H. Lee, P. Bansal, Heat and mass transfer characteristics of a helical absorber using LiBr and LiBr + LiI + LiNO3 + LiCl solutions, Int. J. Heat Mass Transfer 48 (10) (2005) 2102–2109, https://doi.org/10.1016/j.ijheatmasstransfer.2005.01.009.
[15] J. Yoon, E. Kim, K. Choi, W. Seol, Heat transfer enhancement with a surfactant on horizontal bundle tubes of an absorber, Int. J. Heat Mass Transfer 45 (4) (2002) 735–741, https://doi.org/10.1016/S0017-9310(01)00202-2.
[16] S. Lin, Z. Shigang, Experimental study on vertical vapor absorption into LiBr solution with and without additive, Appl. Therm. Eng. 31 (14–15) (2011) 2850–2854, https://doi.org/10.1016/j.applthermaleng.2011.05.010.
[17] Z. B. F. Zhang, X. Li, G. Chen, T. Wang, T. Jin, C. Cheng, G. Li, L. Zhang, F. Zheng, Thermophysical properties and water sorption characteristics of 1-ethyl-3-methylimidazolium acetate ionic liquid and water binary systems Int. Com. Heat Mass Transfer 127 (2021) 105558 https://doi.org/10.1016/j.icheatmasstransfer.2021.105558.
[18] C. W. B. Cao, Y. Yin, F. Zhang, S. Tong, C. Che, Q. Ji, G. Xu, X. Li, Experimental study on heat and mass transfer characteristics between a novel ionic liquid and air under low-humidity conditions Int. J. Heat Mass Transfer 198 (2022) 123373 https://doi.org/10.1016/j.ijheatmasstransfer.2022.123373.
[19] H. Araujo, L. Massuchetto, R. Nascimento, S. Carvalho, J. Dangelo, Thermodynamic performance analysis of a single-effect absorption refrigeration system operating with water and 1-ethyl-3-methylimidazolium based ionic liquids mixtures, Appl. Therm. Eng. 201 (117761) (2022), https://doi.org/10.1016/j.applthermaleng.2021.117761. Part A.
[20] X. Zhang, D. Hu, Performance simulation of the absorption chiller using water and ionic liquid 1-ethyl-3-methylimidazolium dimethylphosphate as the working pair, Appl. Therm. Eng. 31 (16) (2011) 3316–3321, https://doi.org/10.1016/j.applthermaleng.2011.06.011.
[21] M. Królikowska, M. Zawadzki, M. Skonieczny, The influence of bromide-based ionic liquids on solubility of {LiBr (1) + water (2)} system. Experimental (solid + liquid) phase equilibrium data. Part 2, J. Mol. Liq. 265 (2018) 316–326, https://doi.org/10.1016/j.molliq.2018.06.006.
[22] M. Królikowska, T. Hofman, The influence of bromide-based ionic liquids on solubility of {LiBr (1)+water (2)} system. Experimental (solid + liquid) phase equilibrium data.Part 1, J. Molecular Liqs 273 (2019) 606–614, https://doi.org/10.1016/j.molliq.2018.09.104.
[23] D. Latorre-Arca, M. Larrechi, D. Salavera, A. Coronas, A. Rodriguez-Fortea, A. Rivera-Pousa, T. Mendez-Morales, L. Varela, Quantitative and structural analysis of water association in water-lithium bromide-1,3-dimethylimidazolium chloride mixtures, J. Mol. Liqs 368 (2022) 120828, https://doi.org/10.1016/j.molliq.2022.120828. Part B.
[24] V. Soto, J. Pinazo, Validation of a model for the absorption process of H2O(vap) by a LiBr(aq) in a horizontal tube bundle, using a multi-factorial analysis, Int. J. Heat Mass Transfer 46 (17) (2003) 3299–3312, https://doi.org/10.1016/S0017-9310(03)00121-2.
[25] L. Harikrishnan, M. Maiya, S. Tiwari, Investigations on heat and mass transfer characteristics of falling film horizontal tubular absorber, Int. J. Heat Mass Transfer 54 (11–12) (2011) 2609–2617, https://doi.org/10.1016/j.ijheatmasstransfer.2011.01.024.
[26] J. Yoon, T. Phan, C. Moon, H. Lee, S. Jeong, Heat and mass transfer characteristics of a horizontal tube falling film absorber with small diameter tubes, Heat Mass Transfer 44 (2008) 437–444, https://doi.org/10.1007/s00231-007-0261-8.
[27] H. Zhang, D. Yin, S. You, W. Zheng, S. Wei, Experimental investigation of heat and mass transfer in a LiBr-H2O solution falling film absorber on horizontal tubes: comprehensive effects of tube types and surfactants, Appl. Therm. Eng. 146 (2019) 203–211, https://doi.org/10.1016/j.applthermaleng.2018.09.127.
[28] H. Tariq, A. Altamirano, R. Collignon, B. Stutz, A. Coronas, Experimental study on the effect of an ionic liquid as anti-crystallization additive in a bi-adiabatic H2O-LiBr absorption chiller prototype, Appl. Therm. Eng. 259 (2025) 124756.
[29] M. Alvarez, M. Bourouis, Experimental characterization of heat and mass transfer in a horizontal tube falling film absorber using aqueous (lithium, potassium, sodium) nitrate solution as a working pair, Energy 148 (2018) 876–887, https://doi.org/10.1016/j.energy.2018.01.052.
[30] Exploration of ionic liquids or new chemical compunds for improving efficiency of absorption chillers and as heat transfer medium for solar energy harvesting, in: Internal Report, CREVER, Research Group of Applied Thermal Engineering, URV, Tarragona, Spain, 2017.

[31] J. Patek, J. Klomfar, A computationally effective formulation of the thermodynamic properties of LiBr-H2O solutions from 273 to 500K over full composition range, Int. J. Refrig. 29 (4) (2006) 566–578, https://doi.org/10.1016/j.ijrefrig.2005.10.007.
[32] Y.A. Cengel, Heat Transfer, 2nd Edition.
[33] J. Killion, S. Garimella, A review of experimental investigations of absorption of water vapor in liquid films falling over horizontal tubes, HVAC&R Res. 9 (2) (2011) 111–136, https://doi.org/10.1080/10789669.2003.10391060.
[34] S. Kline, F. McClintock, Describing uncertainties in single sample experiments, Mech. Eng. 75 (1953) 3–8.
[35] I. Kyung, K. Herold, Y. Kang, Experimental verification of H2O/LiBr absorber bundle performance with smooth horizontal tubes, Int. J. Refrig. 30 (4) (2007) 582–590, https://doi.org/10.1016/j.ijrefrig.2006.11.005.